

REPORT DOCUMENTATION PAGE

*Form Approved
OMB No. 0704-0188*

The public reporting burden for this collection of information is estimated to average 1 hour per response, including the time for reviewing instructions, searching existing data sources, gathering and maintaining the data needed, and completing and reviewing the collection of information. Send comments regarding this burden estimate or any other aspect of this collection of information, including suggestions for reducing the burden, to Department of Defense, Washington Headquarters Services, Directorate for Information Operations and Reports (0704-0188), 1215 Jefferson Davis Highway, Suite 1204, Arlington, VA 22202-4302. Respondents should be aware that notwithstanding any other provision of law, no person shall be subject to any penalty for failing to comply with a collection of information if it does not display a currently valid OMB control number.

PLEASE DO NOT RETURN YOUR FORM TO THE ABOVE ADDRESS.

1. REPORT DATE (DD-MM-YYYY) 08-10-2008		2. REPORT TYPE Final		3. DATES COVERED (From - To) 01 06 2004 - 31 05 2008	
4. TITLE AND SUBTITLE Multiscale Models of Multifunctional Composites for On-Board Damage Detection and Failure Prevention				5a. CONTRACT NUMBER	
				5b. GRANT NUMBER FA9550-04-1-0402	
				5c. PROGRAM ELEMENT NUMBER	
6. AUTHOR(S) W. A. Curtin				5d. PROJECT NUMBER	
				5e. TASK NUMBER	
				5f. WORK UNIT NUMBER	
7. PERFORMING ORGANIZATION NAME(S) AND ADDRESS(ES) Brown University Division of Engineering Box D, 184 Hope Street Providence, RI 02912				8. PERFORMING ORGANIZATION REPORT NUMBER	
9. SPONSORING/MONITORING AGENCY NAME(S) AND ADDRESS(ES) USAF, AFRL AF Office of Scientific Research 4015 Wilson Blvd, Room 713 Arlington, VA 22203-1954				10. SPONSOR/MONITOR'S ACRONYM(S)	
				11. SPONSOR/MONITOR'S REPORT NUMBER(S) AFRL-SRAR-TR-09-0157	
12. DISTRIBUTION/AVAILABILITY STATEMENT Approved for Public Release, Distribution is unlimited					
13. SUPPLEMENTARY NOTES					
14. ABSTRACT Analytic and numerical models were developed to predict the dependence of electrical resistance on internal fiber damage in carbon-fiber-reinforced polymer (CFRP) composites, so as to make electrical resistance measurement a tool for damage detection and prognosis in CFRP components. The models show that electrical resistance is more sensitive to damage than elastic modulus, that resistance change can be used to detect inadvertent overloads, that the remaining fatigue life after overload cycles can be accurately determined, and that the statistical distribution of electrical resistance changes is narrow enough to permit accurate assessment of the damage state of the material. Macroscopic models of components with damage in the form of holes or delaminations were also developed and their predictions correlated with experimental measurements.					
15. SUBJECT TERMS Composites, Damage, Electrical Resistance, Life Prediction					
16. SECURITY CLASSIFICATION OF:			17. LIMITATION OF ABSTRACT UU	18. NUMBER OF PAGES 10	19a. NAME OF RESPONSIBLE PERSON W.A. Curtin
a. REPORT U	b. ABSTRACT U	c. THIS PAGE U			19b. TELEPHONE NUMBER (Include area code) 401-863-1418

Reset

Multiscale Models of Multifunctional Composites for On-Board Damage Detection and Failure Prevention

Air Force Office of Scientific Research
Grant # FA9550-04-1-0402

Final Report

June 1, 2004 - May 31, 2008

W. A. Curtin, Principal Investigator
Division of Engineering
Brown University, Providence RI 02912

Tel: 401-863-1418 FAX: 401-863-9025 e-mail: curtin@engin.brown.edu

Table of Contents

I.	Background and Motivation	1
II.	Accomplishments	1
	a. Anisotropic Resistance	1
	b. Anisotropic Resistance with Damage	2
	c. Resistance due to Fatigue Damage	4
	d. Continuum-level Damage Modeling	6
	e. Modeling of Multiwall Carbon Nanotubes	8
III.	Summary	9
IV.	Publications	10

I. Background and Motivation

On-board damage assessment and life-prediction, or prognosis, is a key technology for extending the practical mission life of air vehicles and other structural components. In carbon fiber reinforced polymer (CFRP) composites, used for many important structures such as helicopter rotors, fan blades, and pressure vessels, the mechanical deformation and electrical resistance are coupled, suggesting the possibility of real-time sensing that is safer and cheaper than conventional methods. The fact that the electrical resistance of a carbon-fiber composite changes with “damage” has been established by several experimental studies in the last decade [1-4], leading to some empirical correlations. However, the precise nature of the actual damage states giving rise to the resistance change has not been well understood, making the empirical correlations interesting but not directly coupled to predictions of remaining strength or life. To make the electrical response predictive for damage assessment, modeling efforts at various scales are desirable. Usually, composite components are complex, consisting of multiple plies, and have a variety of damage modes. Our work in this project focused on individual unidirectional plies and established the relationship between evolving fiber damage and the anisotropic electrical resistance, which can then be used in computational studies of resistance in damaged multiply laminates and actual components.

Our specific work here built upon several prior advances in both mechanical and electrical modeling by us and collaborators. Direct electro-mechanical modeling of composites under loading was performed by Park et al., who derived an analytical model for the longitudinal resistance change during loading that explained many features seen in their experimental data. Based on an analogy to the mechanical ineffective length, i.e. the length over which a broken fiber recovers stress, Park et al. proposed the existence of a “characteristic electrical ineffective length”, which is the length over which a broken fiber recovers current-carrying capability and is nominally the typical distance between electrical contacts of nearby fibers. Xia et al. built on these ideas to create coupled electrical and mechanical models to describe the longitudinal electrical resistance change due to fiber breaks in continuous fiber reinforced composites under longitudinal tensile loading.

This report discusses the four major accomplishments made in this program toward reaching the goal of application of electrical resistance as a damage monitor in CFRP materials. These accomplishments are described in the sections below. These efforts are fully described in past reports and, more importantly, in a sequence of papers in technical journals. We thus emphasize here the main results, without extensive discussions or analysis that can be found in the publications.

II. Accomplishments

IIa. Anisotropic Resistance

We developed analytic models for the anisotropic electrical resistance of aligned but randomly-touching fibers in a 3 dimensional array. Previous models dealt only with longitudinal resistance, which is trivial in the absence of damage. The transverse resistance, in contrast, depends on the spatial distribution of fiber-fiber electrical contacts and is more subtle. We developed various unit-cell models to predict the transverse resistance as a function of basic material properties, and verified the accuracy of these models against numerical simulations. These models allow for the determination of the

density of internal fiber-fiber electrical contacts from measured data on the longitudinal and transverse resistances. An example of the quality of the predictions versus numerical simulations is shown in Figure 1.

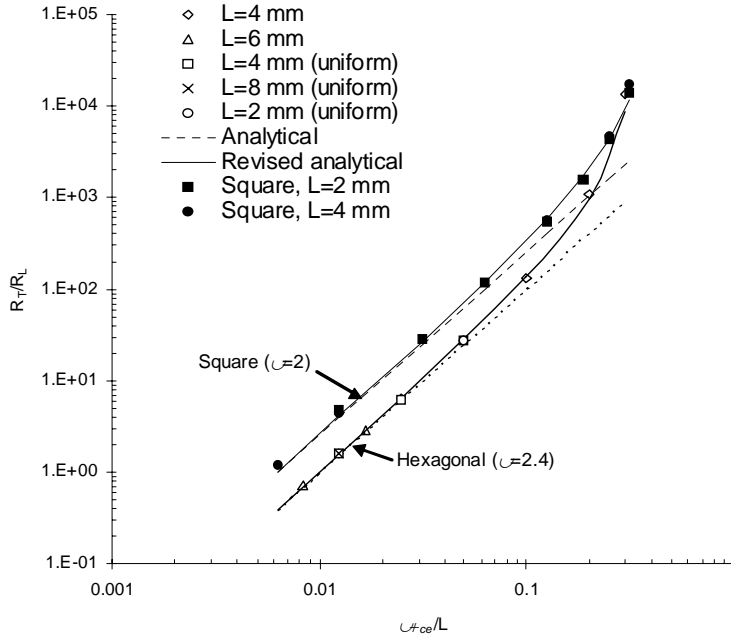


Figure 1. Ratio of transverse resistance to longitudinal resistance R_T/R_L versus normalized fiber contact density parameter $\beta\delta_{ce}/L$ for undamaged composites with two different fiber array types. Note the power-law behavior with exponent 2 (dashed lines) for small $\beta\delta_{ce}/L$, as predicted by the analytical model and the predictions (solid lines) including a finite-size correction.

IIIb. Anisotropic Resistance with Damage

With the resistance of undamaged composite plies established, we turned to the prediction of the electrical resistance as it evolves with mechanical loading, due to fiber damage in the material. The main new result emerging from our analysis is that the functional form of the transverse resistance versus applied strain is *identical* to that for the longitudinal resistance. The differences lie in only two features: the underlying difference in undamaged resistance, which is a simple scaling factor, and a slightly different coefficient associated with the damage rate. The differing coefficients were argued to be due to the difference in transverse and longitudinal current-carrying paths in the fiber electrical network, and their changes upon introducing broken fibers. However, this new damage coefficient, which was estimated analytically, was shown to be largely independent of material properties or fiber contact density and so is a single, robust value for each direction. The analytic models were again confirmed by extensive numerical simulations, and one example is shown in Figure 2.

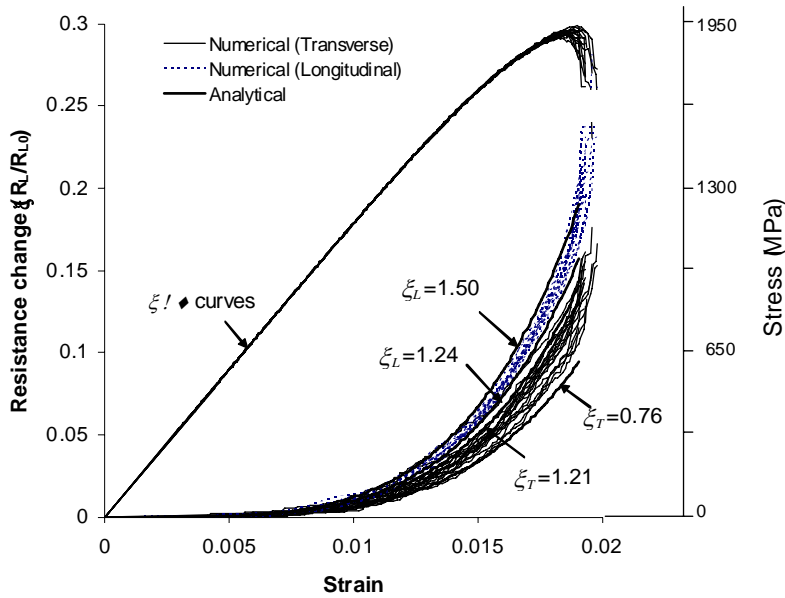


Figure 2. Longitudinal and transverse resistance changes versus applied strain as simulated for 30 different realizations of random fiber-fiber contact distributions, and predictions of the analytical model. The spread in numerical data is captured with a spread in the damage parameter ξ , which is expected to be ~ 1.5 for longitudinal damage and ~ 0.96 for transverse damage. Also shown are the longitudinal stress-strain curves for the same composites.

Of particular interest in practical “damage detection” schemes is the reliability of the measured electrical resistance for predicting the current damage state and/or the remaining strength of the material. We investigated, through extensive numerical analysis, the statistical distribution of the electrical resistance as a function of applied strain. Using a Weibull model, the Weibull modulus (approximately the inverse of the coefficient of variation of the distribution) was found to increase rapidly toward the end of life, implying high reliability in the estimates of damage or strength (Figure 3). The transverse resistance has lower reliability, however, and in general electrical resistance has a broader distribution, even just before failure, than does the mechanical failure strain. This feature arises because of the added disorder in the electrical network due to the fiber/fiber electrical contacts, which does not influence the mechanical response in any way.

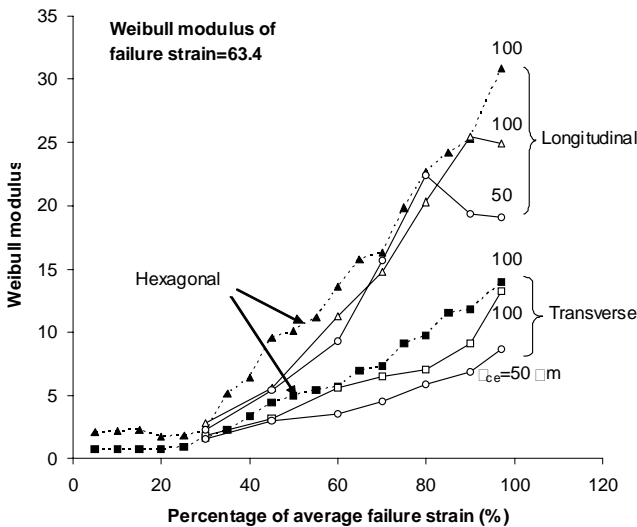


Figure 3. Weibull moduli of transverse and longitudinal resistance distributions versus applied strain.

IIIc. Resistance due to Fatigue Damage

With monotonic loading clearly established above, we then examined the electrical resistance response to damage under cyclic fatigue loading. Here, fatigue is attributed to underlying fatigue crack growth of pre-existing fiber flaws that is represented by a Paris-law model. The fiber fatigue model was validated and calibrated by comparison to experimental data on fatigue of dry bundles of T700S carbon fibers (Figure 4). Analytic predictions of fiber damage and resistance change were for steady cyclic loading and interrupted loading consisting of single-cycle overloads.

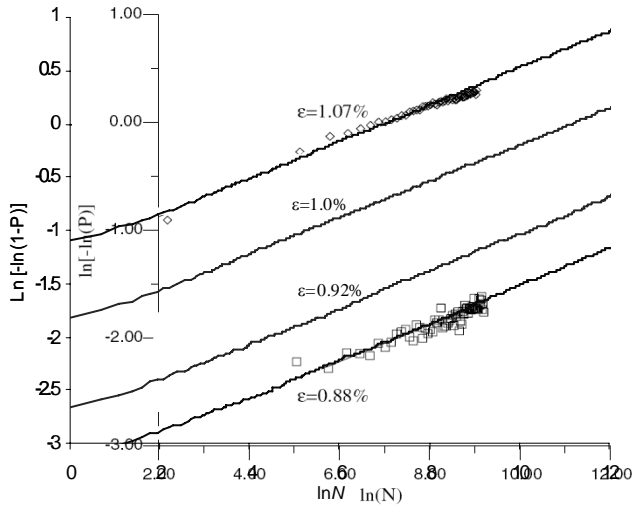


Figure 4. Fiber failure probability versus cycles for T700S fiber bundles under constant strain amplitude cyclic loading. Symbols: experiments; Lines: predictions of an analytic Paris-law model with two Paris-law parameters fit to the data.

The analytic model predicts the resistance versus cycles for arbitrary loading histories. Figure 5 shows the longitudinal resistance predicted by the model and as obtained by numerical simulations for constant-amplitude loading on materials with differing densities of internal fiber contacts and different applied strains; good agreement is evident with no adjustable parameters. The model predicts a correlation between resistance change and stiffness change, with resistance changes being larger in magnitude. Very limited data exists, but our model is in reasonable agreement with that data, demonstrating quantitative relevance to real materials (Figure 6).

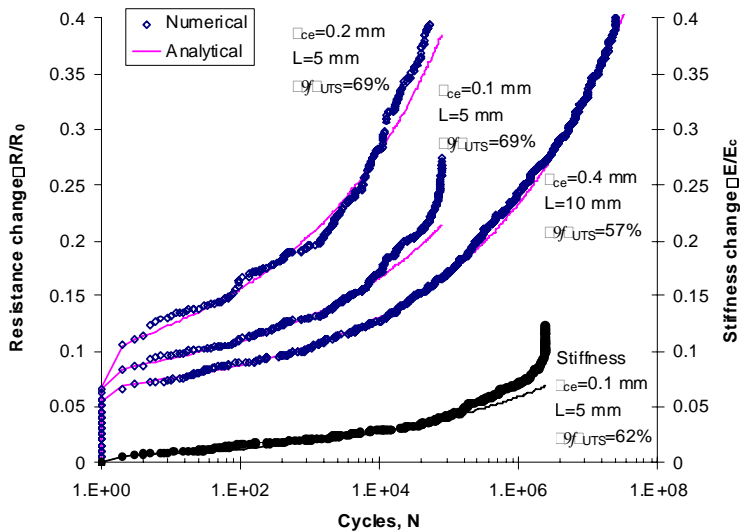


Figure 5. Longitudinal resistance change ($\Delta R/R_0$) as a function of the number of cycles, as predicted by numerical and analytical solutions for various sample lengths L , applied strains normalized by the monotonic failure strain ϵ_{UTS} , and electrical ineffective lengths δ_{ce} .

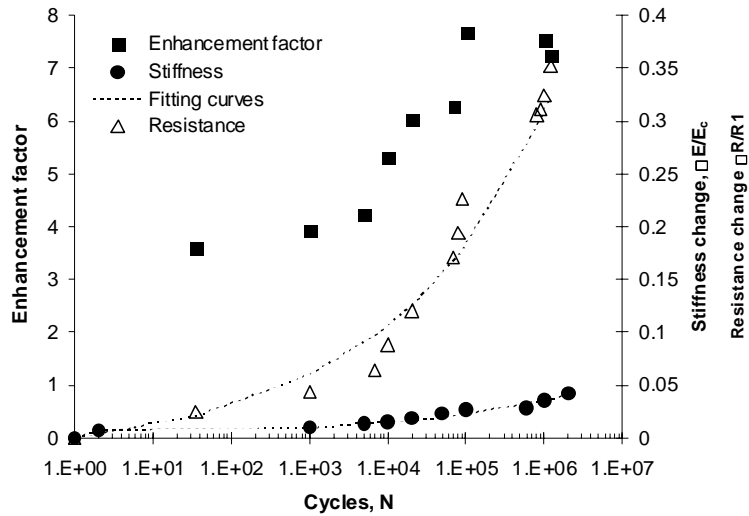


Figure 6. Normalized resistance and stiffness changes during cyclic loading as measured for T300/Hexcel 914 composites. Also shown (right axis) is the experimental enhancement factor, which is predicted by the model to be in the range of 4-6.

Of relevance to prognosis is the remaining fatigue life of the material. We have shown that this can be predicted from the models, and correlates inversely with the resistance change, as shown in Figure 7. The model also accurately accounts for overload cycles, which might arise in application but are outside the scope of the expected mission cycles. Upon one overload cycle, the electrical resistance jumps dramatically, due to the new damage, but then stays relatively constant for many subsequent cycles (Figure 8). This signature could be very useful for after-the-fact detection of overload cycles. We have examined the remaining life of systems having been subjected to an overload cycle, and can predict the life as a function of the overload amplitude and the cycle count at which the overload occurs both in good agreement with numerical simulations. These results demonstrate the flexibility and accuracy of the analytic models.

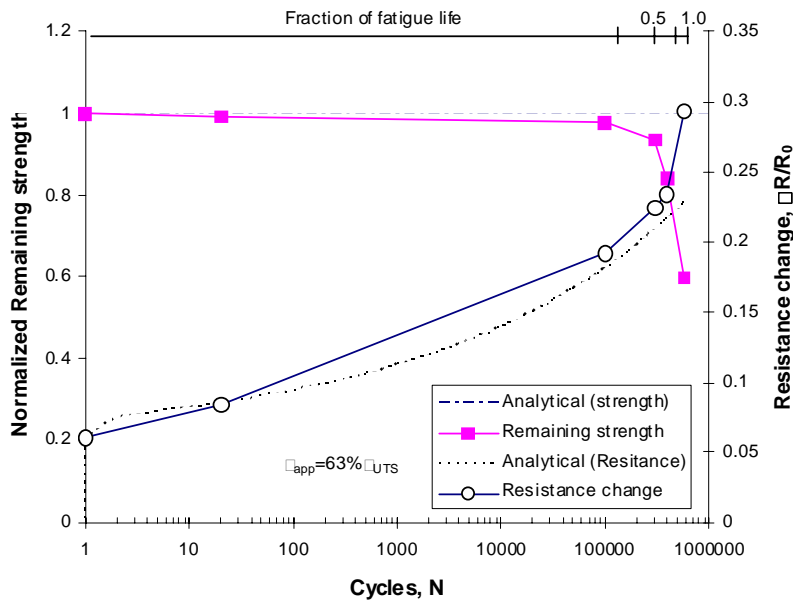


Figure 7. Predicted remaining strength, normalized by initial tensile strength, and resistance change versus number of cycles, for an applied strain amplitude of $\epsilon_{app} = 63\% \epsilon_{UTS}$.

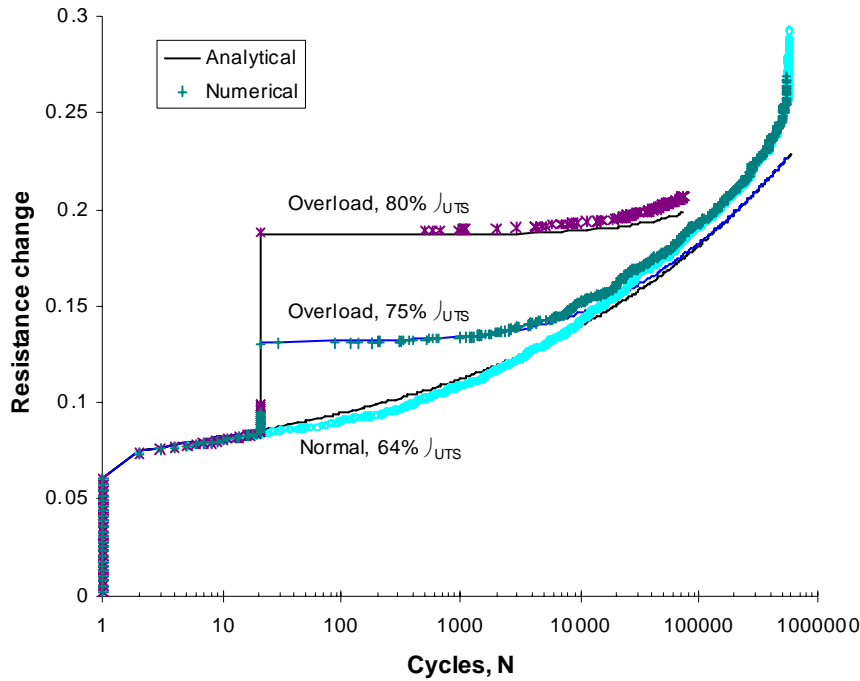


Figure 8. Resistance change versus the number of cycles for at various overload levels relative to the ultimate tensile strain ϵ_{UTS} .

IId. Continuum-level Damage Modeling

In collaboration with Impact Technologies and the University of Dayton Research Institute and funded by an AFOSR STTR program, we developed continuum finite element models to predict the electrical resistance change due to penetration and delamination damages in quasi-isotropic CFRP composite panels. The model consists of electrically anisotropic plies with different orientations and interlayer resistors to represent interlayer impedance. Electrical conductivities of the plies and interlayers are extracted by fitting to experimental data obtained on undamaged specimens. Our previous model (Sec. IIa) relates this macroscopic behavior to the microscopic composite structure. The continuum model was then used to predict electrical resistance changes versus damage size and location. The predicted resistance change is independent of the model-related material constants, a very useful feature for application to various CFRP materials. We applied the model to sample geometries studied by Imact and UDRI (Figure 9). For plates with an array of electrodes on the perimeter, the model successfully predicts those pairs of electrodes that have peak resistance change for a panel with a penetration hole, but with the magnitude of the peak resistances lower than measured in experiments for reasons that can be understood (Figure 10). Predictions for resistance versus electrode location for delamination damage also agree reasonably well with the experiments. To simplify the computations, a quasi-3D model consisting of 2D plies and interlayer impedance was developed and shows results identical to the 3D model but with higher computational efficiency. Overall, these models provide insight into the sensitivity of the resistance changes for various electrode geometries, demonstrating the important role played by the high resistivity anisotropy in these materials. The models could also be used for woven composites, and are useful in tandem

with other damage detection techniques such as neural network to provide “noiseless” data and to verify the results from the neural network.

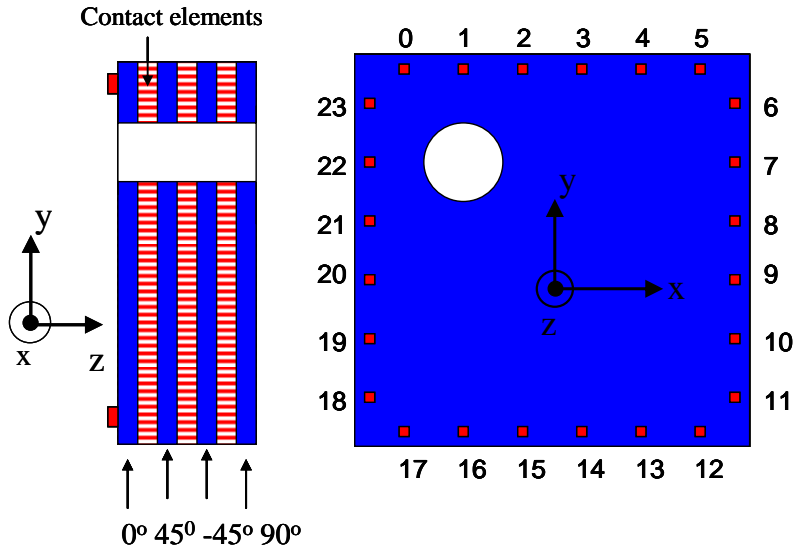


Figure 9. Schematic of composite panel with a 76 mm diameter hole and array of electrical resistance contact points around the perimeter.

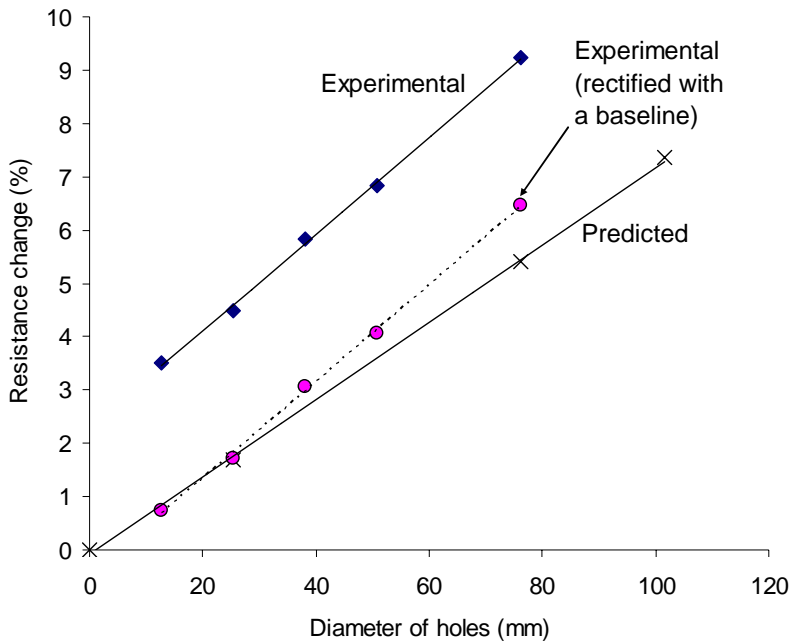


Figure 10. Experimental and predicted average value of peaks in resistance change (in %) as a function of hole diameter.

IIe. Modeling of Multiwall Carbon Nanotubes

Carbon nanotubes (CNTs) are very good electrical conductors and have been used in ceramic matrices to enhance composite electrical conductivity. While being added to polymer composites to improve mechanical strength and toughness, it is also possible that a network of CNTs would provide an electrical resistance that would be sensitive to deformation, damage, or fatigue. Application of CNTs will depend on a range of other material properties. Thus, we were led to work on modeling of realistic Multiwall Carbon Nanotubes (MWCNTs), that is, MWCNTs with interwall sp^3 bonding. Specifically, molecular dynamics (MD) simulations under transverse shear, uniaxial compression, and “pullout” loading configurations were performed for MWCNTs with different fraction of inter-wall sp^3 bonds. The inter-wall shear coupling was shown to have a strong influence on load transfer and compressive load carrying capacity, i.e. buckling resistance. A new continuum shear-coupled-shell model was then developed to predict MWCNT buckling, which agrees very well with all MD results. This work demonstrated that MWCNTs can be engineered through control of inter-wall sp^3 coupling to increase load transfer, buckling strength, and energy dissipation by nanotube pullout, all necessary features for good performance of nanocomposites.

Nanotubes with interwall bonding were constructed, and an example is shown in Figure 11. These samples were subjected to compressive axial loading up until buckling. The buckling strains exceed those of MWCNTs with no interwall bonding because the bonding constrains the relative wall motions and stabilizes the entire nanotube. We derived, in collaboration with Prof. Pradeep Gurudu who also receives AFOSR support through another grant, an expression for the buckling strain as

$$\varepsilon_b = \frac{h}{R\sqrt{3(1-\nu^2)}} + \frac{n-1}{n} \frac{G\delta}{Eh} \quad (1)$$

where R is the nanotube radius, h the height, n the number of walls, G the shear modulus between walls (a function of the sp^3 bond fraction), δ the wall separation, and E the axial Young’s modulus. The first term is the buckling strain of a single wall nanotube, which is enhanced by the shear coupling to other walls (n and G). Figure 12 compares the predicted buckling strain versus the strain measured in MD simulations over a wide of nanotube types. Perfect agreement would correspond to all data points lying on the dashed line of slope unity; the model is in very good agreement with the entire set of MD data points for CNTs with different number of walls SCS model over a large range of η , but fails in the regime of $\eta \rightarrow \infty$, where SCS model continues to work well.

The predictions from our model rationalize experimental results on shell-buckling of individual CVD-fabricated MWCNT. In experiments, the average critical buckling strain was 2.875×10^{-3} , whereas the value for ideal MWCNTs is only 1.725×10^{-3} . Raman spectroscopy analysis on similarly-fabricated MWCNTs shows an sp^3 peak at 1332 cm^{-1} in addition to usual sp^2 peak at 1582 cm^{-1} and the Raman intensity ratio suggests an sp^3/sp^2 ratio of $\approx 0.1-0.4$, equivalent to 1%-6% of inter-wall sp^3 bonds. Using the measured buckling strain and our model, we estimate the effective shear modulus as $G \sim 1.3 \text{ GPa}$ which would correspond to $\sim 0.25\%$ sp^3 bonds, so that quantitative agreement is not obtained by this simple analysis. The difference could lie in the imperfection sensitivity: the experimental buckling strain could be the net result of an increase due to

shear coupling and a decrease due to imperfections. The model thus provides an upper bound for the buckling strain in the presence of inter-wall coupling.

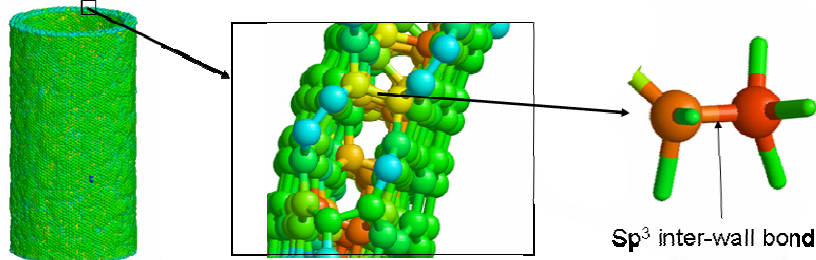


Figure 11. Atomic structure of a CNT with inter-wall sp^3 .

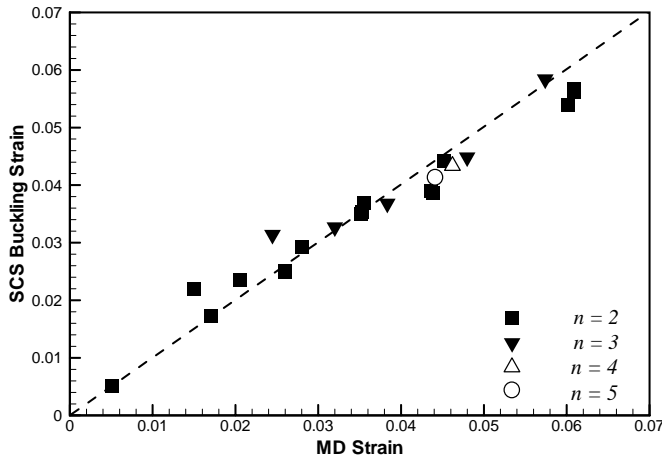


Figure 12. Buckling strain as predicted by the SCS model versus the buckling strain obtained via MD simulations, for a range of MWCNT diameter, percentage of sp^3 bonds, and number of walls.

III. Summary

Our work in this program has advanced the fundamental understanding of electrical resistance in CFRPs by coupling the material response to the detailed material microstructure and material properties. This understanding is encapsulated in a few basic analytic equations whose accuracy has been demonstrated by comparison to detailed numerical simulations. These analytic models thus provide a basis for modeling at the continuum and component levels, and thus are the underpinning scientific foundations for the development of prognosis and life-prediction methodologies in CFRPs.

IV. Publications

1. Z. Xia and W. A. Curtin, "Modeling of Mechanical Damage Detection in CFRPs via Electrical Resistance", *Comp. Sci. Tech.* 67, 1518-1529 (2007).
2. Z. Xia and W. A. Curtin, "Detection of Penetration and Delamination Damage in Quasi-isotropic CFRP Laminates by Electrical Resistance", *Jap. Conf. on Structural Safety and Reliability (JCOSSAR)*, Tokyo, JP, June 2007.
3. Z. H. Xia, P. R. Guduru, and W. A. Curtin, "Enhancing mechanical properties of multiwall carbon nanotubes via sp^3 interwall bridging", *Phys. Rev. Lett.* 98, 245501 (2007).
4. Z. H. Xia and W. A. Curtin, "Fatigue in CFRPs detected using electrical resistance", to appear in *Comp. Sci. Tech.* (2008).
5. Z. Xia and W. A. Curtin, "Multiscale Modeling of Tensile Failure in Fiber-reinforced Composites", in *Multiscale Modeling of Composites*, Springer, (2007).